PHASE-LOCKED RESPONSES IN THE *LIMULUS* LATERAL EYE

THEORETICAL AND EXPERIMENTAL INVESTIGATION

C. ASCOLI, M. BARBI, S. CHILLEMI, AND D. PETRACCHI,
Laboratorio per lo Studio delle Proprietà Fisiche di Biomolecole e Cellule del Consiglio Nazionale delle Ricerche, Pisa, Italy

ABSTRACT The 1:1 phase locking of the neural discharge to sinusoidally modulated stimuli was investigated both theoretically and experimentally. On the theoretical side, a neural encoder model, the self-inhibited leaky integrator, was considered, and the phase of the locked impulse was computed for each frequency in the locking range by imposing the condition that the "leaky integral" $u(t)$ of the driving signal should reach the threshold for the first time one stimulus period after the preceding impulse. As $u(t)$ can be a nonmonotonic function, this approach leads to results that sometimes differ from those reported in the literature. It turns out that the phase excursion is often much smaller than the value of about 180° predicted from previous analyses. Moreover, our analysis shows a peculiar effect; the phase locking frequency range narrows when the input modulation depth increases. The theoretical predictions are then compared with phase-locked discharge patterns recorded from visual cells of the *Limulus* lateral eye, stimulated by sinusoidally modulated light or depolarizing current. The phases of the locked spikes at each of a number of modulation frequencies have been measured. The predictions offered by the model fit the experimental data, although there are some difficulties in determining the effective driving signal.

INTRODUCTION

In the neural cells the external stimulus is first transduced into an internal signal, i.e. the membrane depolarization called "generator potential." This signal, a continuous one, is then converted into a train of all-or-none pulses, which carry information. It has been shown that these two processes are anatomically separate (Tomita, 1957; Fuortes, 1962; Purple and Dodge, 1965).

This paper considers the second process. Neural encoding was first studied as a linear process, leading experimentally to the determination of its transfer functions in many preparations. On the theoretical side, the first type of neural encoder model to be studied was a very simple one, the integrate-and-fire system (Bayly, 1968; Knight, 1969; Stein et al., 1972); here a pulse is fired whenever the integral of the input signal reaches a threshold value, the integration starting with the previous pulse. In this model the output spike density is an exact replica of the input signal (Knight, 1969).

More recently, interest in the nonlinearities of the neural encoding process has rapidly increased; the linear approach to the study of the behavior of neural cells is, in

fact, only a first approximation. Much experimental evidence showing clear nonlinear responses recorded from receptor neurons has been reported (Poppele and Bowman, 1970; French et al., 1972; Poppele and Chen, 1972). In particular, some recent results obtained by recording the activity of light-adapted ommatidia in the *Limulus* lateral eye show that neural encoding in this preparation is markedly nonlinear: even for modulation depths as low as 5%, the spikes synchronize on the sinusoidally modulated stimulus; that is, they occur only within a fixed phase interval of the stimulus cycle (Ascoli et al., 1974). Moreover, completely phase-locked responses, where one spike always occurs in each cycle at the same phase of the stimulus and where the spike rate is entrained by the stimulus frequency, can be recorded in the same preparation by modulating the stimulus signal at frequencies close to the discharge rate in absence of modulation (Knight, 1972*a*; Ascoli et al., 1976).[1]

On the theoretical side, encoder models more realistic than the integrate-and-fire model have been proposed and analyzed. The leaky integrator is a slightly more complex model that accounts for some typical nonlinear features of neural cells, such as the threshold depolarization necessary to elicit a sustained discharge and the phase locking of the spikes to a cyclic stimulus. Rescigno et al. (1970) analyzed this model, dealing specifically with the phase-locked discharge patterns it produces on cyclic inputs, while Knight (1972*b*) fitted the model to the resonant amplification of the spike density response occurring in the eccentric cell of the Limulus lateral eye, at modulation frequencies near the free-run discharge rate.

In this paper we analyze the 1:1 phase-locking behavior of the leaky integrator and compare the theoretical predictions with empirical phase-locked responses recorded from *Limulus* lateral eye visual neurons. A theoretical analysis of phase-locking for this model has been developed in two previous papers (Rescigno et al., 1970; Knight, 1972*a*). But as we show below, this analysis is reliable only if the driving signal always remains above the threshold value for steady firing. Now, in experimental recordings from neural cells, it is often difficult to check if that condition holds. In the preparation we used, owing to the self-inhibitory feedback of the discharge on itself (Stevens, 1964; Purple and Dodge, 1965), the effective driving signal is due to the combination of the generator potential with the self-inhibitory potential; only the first of these can be measured experimentally. Our analysis therefore examines the phase-locking behavior for every stimulus level and takes into account the self-inhibitory feedback too. The theoretical predictions can thus be compared with the experimental data from the *Limulus* visual cells.

THEORY

Leaky Integrator Model

Let us first consider the simple leaky integrator model, without self-inhibitory feedback, defined as follows: whenever the "leaky integral" $u(t)$ of the input signal $s(t)$

[1]It is worth noting that here the term "phase locking" is used only in the strict sense just defined, whereas it has often been used as a synonym for phase preference or even modulation of the response.

reaches a constant threshold C, a pulse is fired and u is instantaneously reset to zero; in the interpulse interval, the input signal determines the u function according to the equation

$$du/dt = -\gamma u(t) + s(t), \tag{1}$$

where γ is the leakage constant. Thus $u(t)$ is not always a monotonic time function, its derivative being negative when $u(t) > s(t)/\gamma$.

For a constant stimulus $s = s_0$, the solution of Eq. 1 is $u(t) = (s_0/\gamma)(1 - e^{-\gamma t})$. The steady-state relation is therefore (Knight, 1972*a*):

$$s_0(1 - e^{-\gamma/f_0}) = \gamma C, \tag{2}$$

where f_0 is the rate of discharge.

We restrict ourselves to input signals of the form $s(t) = s_0(1 + m\cos 2\pi\nu t)$, with $m < 1$ and $s_0 > \gamma C$, which is the minimum depolarization needed to elicit firing in steady conditions (Eq. 2). The leaky integrator model can generate phase-locked pulse trains when driven with such input signals. In particular, for modulation frequencies ν near the free-run impulse rate, one impulse occurs in each cycle, always in the same position on the input sinusoid (Knight 1972*a*; Rescigno et al., 1970).

It is this 1:1 phase locking that interests us. The phase of the locked impulses can be computed for each frequency by imposing the condition that $u(t)$ should reach the threshold C for the first time after exactly one stimulus period. From Eq. 1 we have

$$u(t) = \int_0^t s(t')e^{-\gamma(t-t')}\,dt', \quad \text{or} \quad u(t) = \int_0^t s_0(1 + m\cos(\omega t' + \varphi))e^{-\gamma(t-t')}\,dt',$$

where $\omega = 2\pi\nu$ and φ is the phase at which the last impulse has occurred. Integration by parts gives:

$$u(t) = (s_0/\gamma)(1 - e^{-\gamma t}) + (s_0/\gamma)m\cos\beta[\cos(\omega t + \varphi - \beta) - e^{-\gamma t}\cos(\varphi - \beta)], \tag{3}$$

where $\beta = \tan^{-1}(\omega/\gamma)$ $(0 \le \beta \le \pi/2)$. Now, for the interpulse interval to coincide with the stimulus period ν^{-1}, the expression

$$u(\nu^{-1}) = (s_0/\gamma)(1 - e^{-\gamma/\nu})[1 + m\cos\beta\cos(\varphi - \beta)], \tag{4}$$

must be equal to the threshold C, giving the equation:

$$\cos(\varphi - \beta) = (\sqrt{\gamma^2 + \omega^2}/\gamma m)\{\gamma C/s_0(1 - e^{-\gamma/\nu}) - 1\},$$

or, by using Eq. 2:

$$\cos(\varphi - \beta) = \frac{\sqrt{\gamma^2 + \omega^2}}{\gamma m}\left(\frac{1 - e^{-\gamma/f_0}}{1 - e^{-\gamma/\nu}} - 1\right). \tag{5}$$

Using this equation, Rescigno et al. (1970) and Knight (1972*a*) determined the phase φ of phase-locked impulses. However, this phase is a true phase-locking phase only if $u(t)$ has not already been equal to C within the time interval $(0, \nu^{-1})$ (see Fig. 1). A

sufficient condition for this is that the modulation depth m should be less than $1 - \gamma C/s_0$,[2] so that the stimulus $s(t)$ never falls below the threshold value for steady firing γC. In fact, point A in Fig. 1 satisfies the conditions $u = s - \gamma u < 0$ and $u = C$, so that $s < \gamma C$. The condition $s(t) > \gamma C$ for each time t in the interval $(0, \nu^{-1})$ therefore ensures that the solution φ of Eq. 5 is acceptable as a phase-locking phase. But when $s(t)$ falls below γC in some part of the interval, the solution of Eq. 5 must always be checked to see whether it is a first-crossing solution.

With this proviso in mind, we shall now investigate in detail the existence and behavior of solutions of Eq. 5. The expression in parentheses on the right-hand side of Eq. 5 vanishes for $\nu = f_0$. Thus in a frequency range containing f_0, the absolute value of the right-hand side of Eq. 5 is less than one; moreover, if m is sufficiently small, this range is delimited by the frequencies $\nu_{\min}$ and $\nu_{\max}$, such that the right-hand side of Eq. 5 equals -1 or $+1$, respectively (see Appendix). Clearly, Eq. 5 has two solutions for φ for each value of ν in this range. Let us call φ_1 the solution yielding $\sin(\varphi - \beta) < 0$ and φ_2 the other one.

Let us now decide which solution[3] corresponds to a stable phase-locking position, i.e. such that a small displacement—one, for instance produced by noise—of the spike from the locking phase causes a compensating variation in the successive interval (thus the delaying of a spike leads to a shortening of the successive interval).[4] For the unstable phase, on the other hand, any perturbation is followed by a further removal from the locking phase. It is clear that in biological systems, where there is always some intrinsic noise, only stable phase-locking can be observed. Now, on account of the preceding definition, stable phase locking corresponds to a positive value for the derivative $\partial u(T)/\partial\varphi$. In fact an increase in φ is equivalent to a delay in the first spike, while an increase in u produces a shorter interval. By computing the derivative of expression 3 with respect to φ, the stability condition becomes:

$$-m(s_0/\gamma \cos\beta(1 - e^{-\gamma/\nu}) \sin(\varphi - \beta) > 0$$

or, since the other factors must be positive:

$$\sin(\varphi - \beta) < 0. \tag{6}$$

Therefore, only solution φ_1 corresponds to stable phase locking.

So, if m is low enough, real phase locking occurs for each frequency in the range $(\nu_{\min}, \nu_{\max})$; with increasing ν in this range, the locking phase φ_1 increases continuously from the value $\tan^{-1} 2\pi\nu_{\min}/\gamma - \pi$ to $\tan^{-1} 2\pi\nu_{\max}/\gamma$, with an excursion of about (but slightly over) 180°. For larger modulation depths, such that $s(t)$ falls below the value γC in some part of the cycle, a check must be carried out to see whether φ_1 is a first crossing solution of Eq. 5; we did this by numerically computing the corresponding

[2]Note that from the steady relation (Eq. 2): $1 - \gamma C/s_0 = e^{-\gamma/f_0}$, which decreases exponentially with increasing γ.

[3]We expect one solution and only one to represent a stable phase-locking position, since if both were stable (or unstable), two intermediate unstable (or stable) positions would also exist.

[4]The "monotonicity" of the leaky integrator model (Knight, 1972 *a*) ensures that this compensation cannot in any case exceed the original displacement.

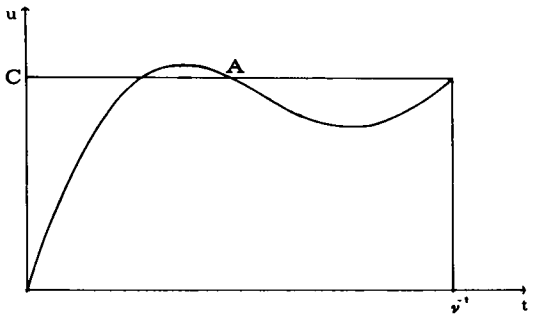

FIGURE 1

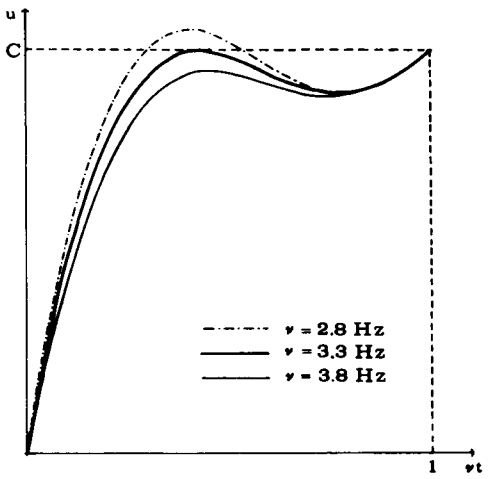

FIGURE 2

FIGURE 1 $u(t)$ function corresponding to a solution of Eq. 6 that is not a first crossing solution. Parameter values: $f_0 = 5$ spikes/s, $\gamma = 16\,s^{-1}$, $m = 0.4$, $\nu = 3.4$ Hz.
FIGURE 2 $u(t)$ function corresponding to the solution of Eq. 6 for three different modulation frequencies; other parameter values: $f_0 = 5$ spikes/s, $\gamma = 16\,s^{-1}$, $m = 0.2$.

function $u(t)$, as given by Eq. 3. It turns out that for $\nu = \nu_{max}$ the solution is really a phase-locking phase, whereas as the frequency is decreased, the function $u(t)$ presents a relative maximum that rises with decreasing ν. The frequency at which this maximum reaches C is actually the lower end of the locking range. This behavior is shown in Fig. 2. Finally, in Fig. 3 we have plotted the phase of real phase locking vs. ν for several modulation depths and two different values of the ratio γ/f_0 (clearly the solution of Eq. 5 depends only on the dimensionless variables γ/f_0 and ν/f_0).

Fig. 3 shows that when m is increased, the phase excursion becomes smaller than 180° and the frequency range becomes asymmetrical with respect to f_0 in the direction of high frequencies. Moreover there are frequencies where an increase of the input modulation depth causes the loss of the 1:1 phase-locking condition (see the frequency range between the arrows).[5] These effects depend on the above-discussed behavior of the $u(t)$ function. At the lower value of γ/f_0 (1.6) the effects arise for higher modulation depths than at the higher one (3.2).

Leaky Integrator with Self-Inhibitory Feedback

To introduce self-inhibitory feedback into the model, we only have to replace the stimulus $s(t)$ by the difference $s(t) - I(t)$ in the integral form of $u(t)$ where $I(t)$ is the self-inhibitory potential. This is built by adding, at the moment of each spike, an increment A_s, which then decays exponentially with time constant τ. Since our analysis

[5]Using an electronic analogue of the model, we found that when 1:1 phase locking is lost, a more complicated phase locked pattern occurs: for instance a 3:2 pattern (three impulses every two cycles) followed, by further increasing m, by a 5:3 one, a 2:1, etc.

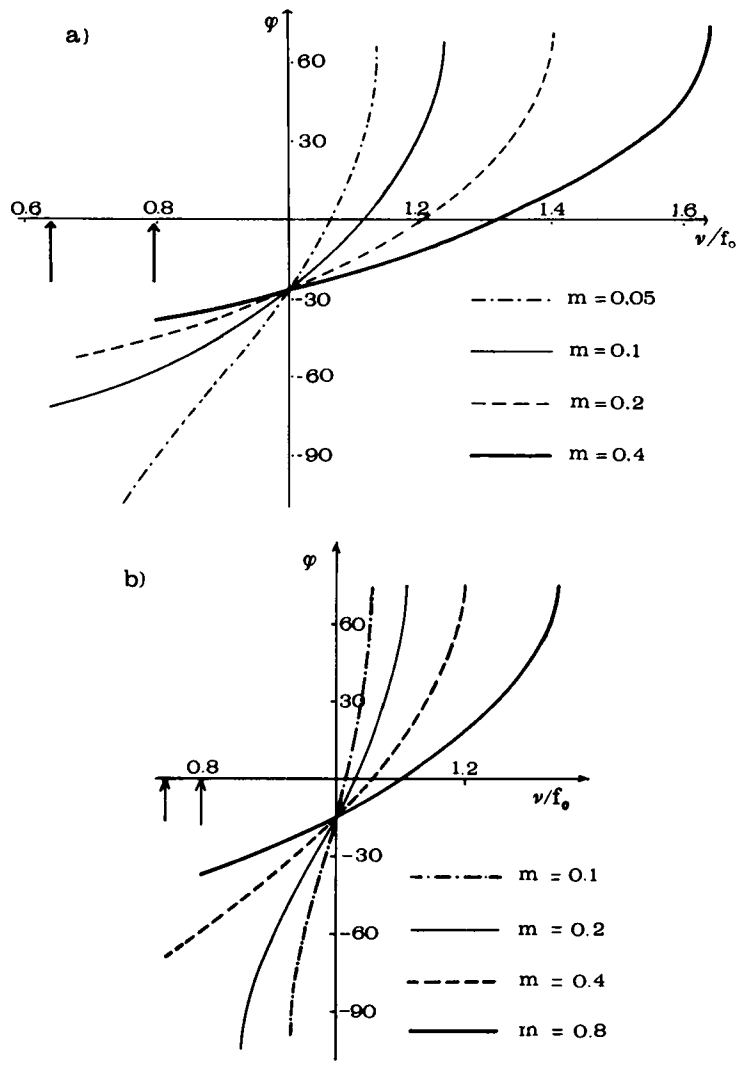

FIGURE 3 $\varphi(\nu)$ function predicted by the leaky integrator: (*a*) $\gamma/f_0 = 3.2$, (*b*) $\gamma/f_0 = 1.6$.

is confined to phase-locked patterns, $I(t)$ turns out to be a pseudo-stationary inhibitory potential; after every spike it reaches the value $A_s/(1 - e^{-T/\tau})$, where T is the interspike interval. Therefore: $I(t) = A_s e^{-t/\tau}/(1 - e^{-T/\tau})$. Computing the integral relative to the added term is trivial and leads to the phase-locking equation:

$$\cos(\varphi - \beta) = \frac{\sqrt{\gamma^2 + \omega^2}}{m\gamma}\left[\frac{\gamma C}{s_0(1 - e^{-\gamma/\nu})} - 1 + \frac{KC\gamma}{s_0(\gamma\tau - 1)}\left(\frac{1}{1 - e^{-1/\tau\nu}} - \frac{1}{1 - e^{-\gamma/\nu}}\right)\right], \quad (7)$$

where $K = A_s\tau/C$.

It again happens that two solutions exist for any frequency ν within a range containing f_0; they differ for the sign of sin $(\varphi - \beta)$. As before let us call φ_1 the solution corresponding to sin $(\varphi - \beta) < 0$. We first note that the solutions φ_1 and φ_2 do not coincide for every value of cos $(\varphi - \beta)$ different from -1 or $+1$. Moreover, for reasons of continuity, the same solution always corresponds to a stable phase locking with varying ν, and also if the strength A_s of self-inhibition is varied. Thus, for the self-inhibited model too, we expect φ_1 to be the stable phase. On the other hand, it is very hard to carry out an analytical study of the stability in this case; we have therefore checked our conclusion by simulating the model with an electronic analogue. In fact, the stable phase is φ_1, as when there is no self-inhibition.

As in that case, this approach is only reliable if the driving signal $s(t) - I(t)$ is always greater than γC. Otherwise the solutions obtained must be numerically checked to be first crossing solutions. In Fig. 4 we report the function $\varphi(\nu)$ for some values of K, τ, and γ. In this case we have chosen not to use the underlying dimensionless variables to simplify the comparison between theoretical predictions and experimental data. It is worth noting that the self-inhibitory feedback does not introduce new qualitative features in the $\varphi(\nu)$ trend. As before, when the modulation depth increases, the range of the phase-locking phase becomes smaller than 180°, and the frequency range becomes displaced with respect to f_0 towards higher frequencies (the asymmetry increasing with m). Moreover, there are frequencies at which phase locking is lost with increasing input modulation depth.

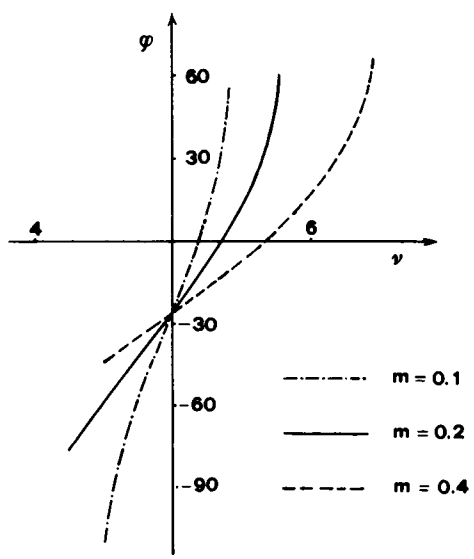

FIGURE 4 $\varphi(\nu)$ function predicted by the self-inhibited leaky integrator. Parameter values: f_0 = 5 spikes/s, $\gamma = 16\,s^{-1}$, $K = 2$, $\tau = 0.5$ s, and modulation depths as quoted.

EXPERIMENTAL APPROACH

The experiments reported below were carried out to obtain quantitative measurements of phase-locked responses against which to test the theory described above. In this connection the relevant quantities are: (*a*) the locking phase at the frequency of the free-running discharge, $\varphi(f_0)$, which would depend only on the leakage constant (see Eq. 7); (*b*) the phase excursion $\Delta\varphi = \varphi(\nu_{max}) - \varphi(\nu_{min})$, swept by φ as the stimulation frequency is varied. In previous analyses of the model, $\Delta\varphi$ is always about 180°, while in our treatment it can be much lower. The precise (always increasing) trend of $\varphi(\nu)$ has been predicted theoretically, too. Note that φ is the phase-shift of the spike from the maximum of the driving signal.

Electrophysiological experiments were performed on the *Limulus* lateral eye visual neurons. Recordings from retinular and eccentric cells were made while sinusoidally modulating the stimulus at frequencies near the discharge rate in the absence of modulation, in order to get phase-locked responses. Now, in the presence of light stimulation, two processes are performed in these visual cells: transduction of light into generator potential, and encoding of generator potential into spike trains. The encoding process is known to occur in the axon hillock of the eccentric cell (Purple and Dodge, 1965; Tomita, 1957); nevertheless the spikes invade the cellular body electrotonically, and as a result of the electrical coupling, can be recorded from the retinular cells too. As regards the generator potential, simultaneous recordings from pairs of visual cells in the same ommatidium (Smith and Baumann, 1969) show no appreciable delay between the time-courses of the generator potentials recorded in retinular cells and the eccentric one. Therefore it should be possible to study the neural encoding process by recording from retinular cells too and, in our case, by measuring the phase of the locked spikes with respect to the generator potential. In the responses of retinular cells that we have analyzed, spikes of the amplitude of a few millivolts appeared superimposed on the modulated generator potential, so that the phase of the spike with respect to the generator potential could be directly measured. Current stimulation has also been used; in this case the current itself is generally assumed to be the signal driving the discharge (Knight et al., 1970), and we therefore measured the phase of the spikes with respect to the modulated current.

METHODS

The Biological Preparation

Limulus poliphemus specimens with a 4–6-inch carapace were sent by air from the Marine Biological Laboratory (Woods Hole, Mass.) in a moist barrel. As soon as they arrived, the animals were put in a pond with circulating aerated sea water and fed fresh mussels. During the journey about 10% of the animals died, but the survivors soon showed apparently good health. Experiments were performed on excised lateral eyes. The eye was drawn out with a small carapace frame and split horizontally along the major axis of the ommatidium with a small microtome. The inferior half of the eye was mounted in a small chamber, with the carapace frame clamping it, with the exposed tissue facing upwards. The chamber was filled with just

enough seawater to cover the cut. The experiments were performed at room temperature (about 20°C).

Recording Technique

Micropipettes filled with 2.7 M KCl having resistances between 5 and 50 MΩ were used to impale the visual neurons. The micropipette, held by a Leitz micromanipolator (E. Leitz, Inc., Rockleigh, N.J.), was lowered under visual control. Cells belonging to exposed ommatidia, or to ommatidia immediately below these, were impaled. Recordings were taken from eccentric cells or retinular cells with distinguishable spikes; the cells were assigned to one of these two classes according to the features of spikes and generator potential observed (retinular cells, small spikes and high generator potential; eccentric cells, large spikes and low generator potential). Electrical connections to the micropipette were made by Ag-AgCl electrodes. The reference electrode was another Ag-AgCl wire, which made contact with the extracellular fluid by an agar bridge. The electronic arrangement used for recording consisted of a unity-gain preamplifier with capacitance neutralization and a bridge circuit that made it possible to balance the potential drop across the electrode resistance when current was passing through the cell. Resting potentials in the 30–50 mV range were typically found in retinular cells and slightly higher ones in eccentric cells; cell impedances (not always measured) were about 5 MΩ. These values were maintained during the course of each experiment with a minimum drift. Cells firing when put in the dark were discarded.

Stimulus Features

The activity of the impaled cells was recorded on magnetic tape after adaptation to the steady level of the stimulus used. The mean rate of firing was then always below 10 spikes/s. As a rule, this rate slowly declined throughout the experiment. Only the runs with nearly stable firing rates were analyzed. Sinusoidally modulated light or depolarizing current were used to stimulate impaled cells. In some cases, however, a steady light and a sinusoidal current were applied simultaneously to modulate the activity of the cells around a level of excitation produced by the natural stimulus. This system may be called "hybrid stimulation." The modulation depth m of a sinusoidally modulated signal is defined, as under Theory, as the dimensionless ratio between half the peak-to-peak amplitude of the signal and its mean value.

For the current stimulus, m was selected on the stimulating device. For the recordings with light stimulation, the modulation depth of the generator potential was measured, when possible, on the recorded signal.

Lastly, for hybrid stimulation, the generator potential excursion was estimated as the product of the measured impedance of the cell and the amplitude of the sinusoidal current. The single ommatidium was illuminated with an optical fiber 50 μm in diameter touching the cornea. That the impaled cell did not fire when the light stimulus was applied to a contiguous ommatidium proved the selectivity of the stimulation. The light source was a 100-W tungsten-halogen lamp. The total light power leaving the fiber had a maximum value of about 0.1 μW. An electromechanical device provided with feedback control allowed varying light levels and modulation depth.

Data Analysis

The cycle histograms reported in the text were obtained by means of a signal processor, the Laben Correlatron 1024 (LABEN, Milano, Italy). This processor produces cycle histograms by dividing every cycle into equal consecutive time bins of preset duration and counting the number of spikes occurring in each bin, over many input cycles. The time duration of the reported cycle histograms is one full cycle.

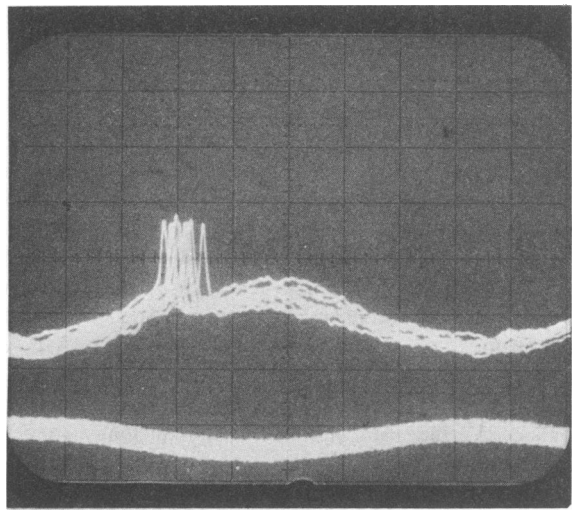

FIGURE 5 Phase locked discharge pattern: several sweeps were superposed on the screen of the storage oscilloscope synchronized with the stimulus. The phase of the locked spikes can be obtained by estimating its average distance from the maximum of the generator potential. The lower trace represents the light stimulus. Calibrations: 35 ms/div, abscissa; 2 mV/div, ordinates. Resting potential and zero stimulus level correspond to the lower edge of the picture.

For the cycle histograms of responses to light stimulation, the processor was triggered at every maximum of the light. At the frequencies used, generator potential is about 180° out of phase with respect to the light stimulus (Knight et al., 1970). This implies that the generator potential maximum occurs near the center of the histograms.

In any case the phase of the locked spikes with respect to the modulated generator potential was estimated directly from pictures of the patterns obtained on the screen of a storage oscilloscope synchronized with the stimulus signal (Fig. 5). The phases were measured from the maximum of the generator potential, located by fitting a sinusoid against the generator potential waveform.

In the case of current stimulation, the phase of locked spikes with respect to current can be accurately measured on the cycle histograms. The cycle histograms of responses to current stimulation start from the minimum of the current ($\varphi = -180°$). The delay in detection of the spikes by the processor was taken into account in the phase measurements. Wherever possible, about 120 cycles were taken to generate the cycle histograms.

RESULTS

Fig. 6 shows the cycle histograms of responses of a retinular cell to sinusoidally modulated light impinging on the impaled ommatidium. The firing rate of the cell when stimulated by unmodulated light (free-run rate f_0) declined slowly from 5.3 spikes/s at the beginning of the recording to 5.1 spikes/s at the end.

All the histograms consist of a single peak. The narrowest peaks appear in the histograms at 5 and 5.4 Hz, 10% modulation depth of the light, and those at 5 Hz, 5.3 Hz and 5% modulation depth, which are also the nearest to the free-run rate. They correspond to discharge patterns where one spike is fired in each stimulus cycle, always at

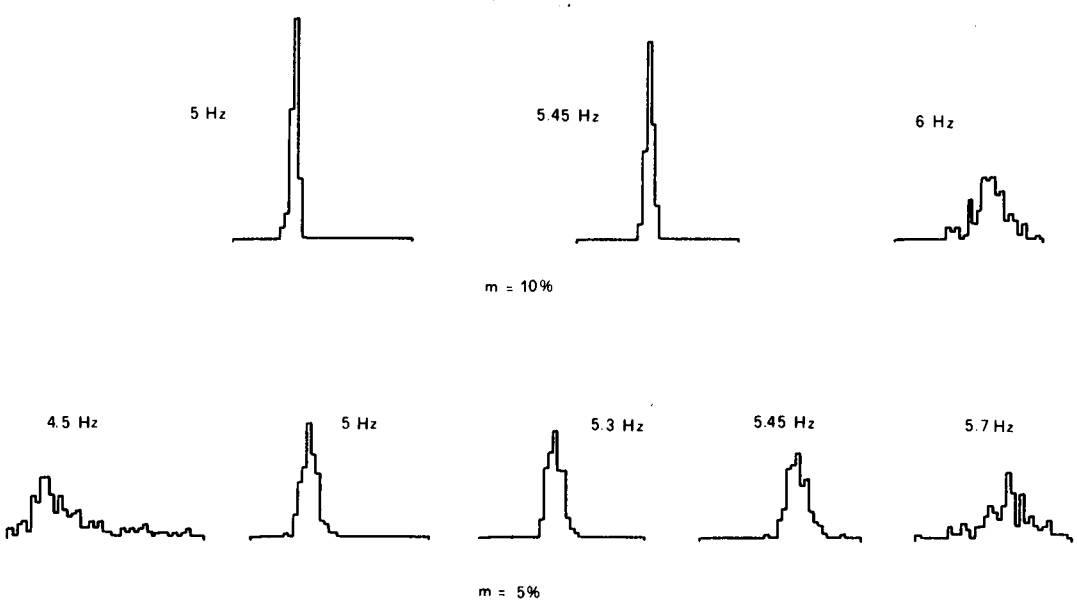

FIGURE 6 Cycle histograms of responses of a retinular cell to 5 and 10% modulated light. The histograms start from the maximum of the light stimulus. About 120 cycles were averaged for each histogram. Time bin: 5 ms. f_0 . 5.2 spikes/s.

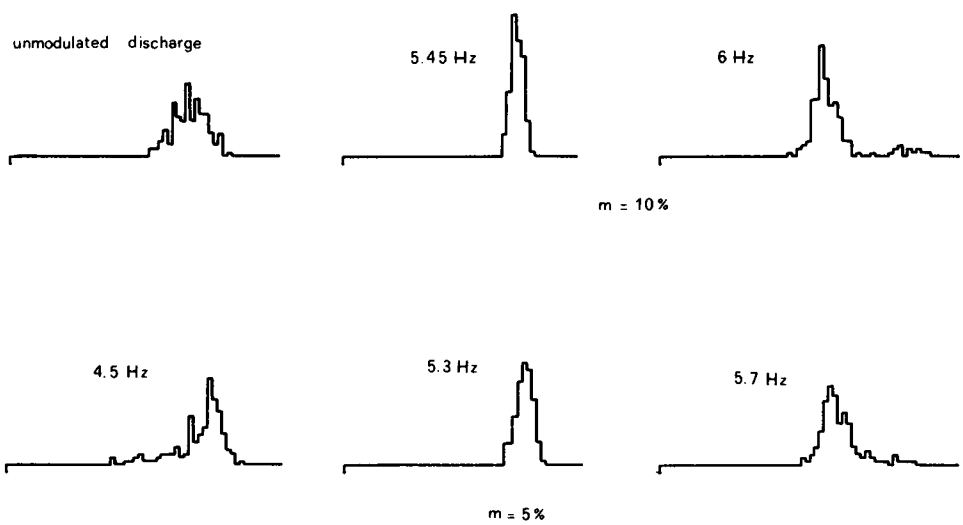

FIGURE 7 Interval histograms for the unmodulated discharge and some of the runs of Fig. 6. Time bin: 5 ms.

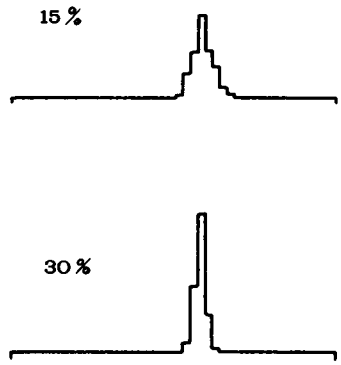

FIGURE 8 Cycle histograms of the responses to light modulated at a frequency very near f_0. Generator potential modulation depths were as marked. f_0 = 7.4 sp/s. Time bin: 3 ms.

about the same phase so that the firing rate is exactly equal to the modulation frequency; in this case we consider the discharge to be exactly phase-locked with the stimulus signal. For stimulation frequencies farther away from f_0 or, at a given frequency, for lower modulation depth (see the two histograms at 5.45 Hz), the peaks in the histograms get broader and broader. As can be seen by visual inspection on the screen of the oscilloscope synchronized with the stimulus signal, the discharge patterns still tend to phase lock on the stimulus, with partial entrainment of the discharge rate. For instance, at 5.45 Hz and 5% modulation depth, the mean firing rate is about 5.3 spikes/s, against a free-run rate of about 5.1 spikes/s; the spike tends to fire at a given phase but there is an increasing delay until the spike falls behind by a full cycle; the spikes are allowed only one phase interval, which they sweep cyclically. Some features of the modulated discharge are better displayed by the interval histograms. These are shown in Fig. 7 for the same runs of Fig. 6. The histograms of exactly phase-locked responses are narrower than those for the unmodulated discharge, while, at frequencies where only partial entrainment occurs, the interval histograms become broader and asymmetric (m = 5%) or even bimodal (m = 10%). The same qualitative features appear in all the responses we recorded; phase-locked responses can be obtained in almost all cells, although difficulties may be encountered in very noisy cells.

Another general feature appearing in all the recordings (obtained during light or current stimulation) is that the phase-locking phase is independent of the stimulus modulation depth for $\nu = f_0$ (Fig. 8), whereas it is dependent on it when ν is different from f_0.

Fig. 9 shows the cycle histograms of responses of another retinular cell stimulated by sinusoidally modulated light with several modulation depths. For the lower modulation depth (corresponding to 5% in the generator potential), the shape of the cycle histograms shows that firing occurs with a strong phase preference, but without a complete entrainment of the firing rate from the stimulation frequency. At the intermediate modulation depth there is, instead, a true phase locking with complete entrainment. The responses for the higher modulation depth illustrate the typical effect

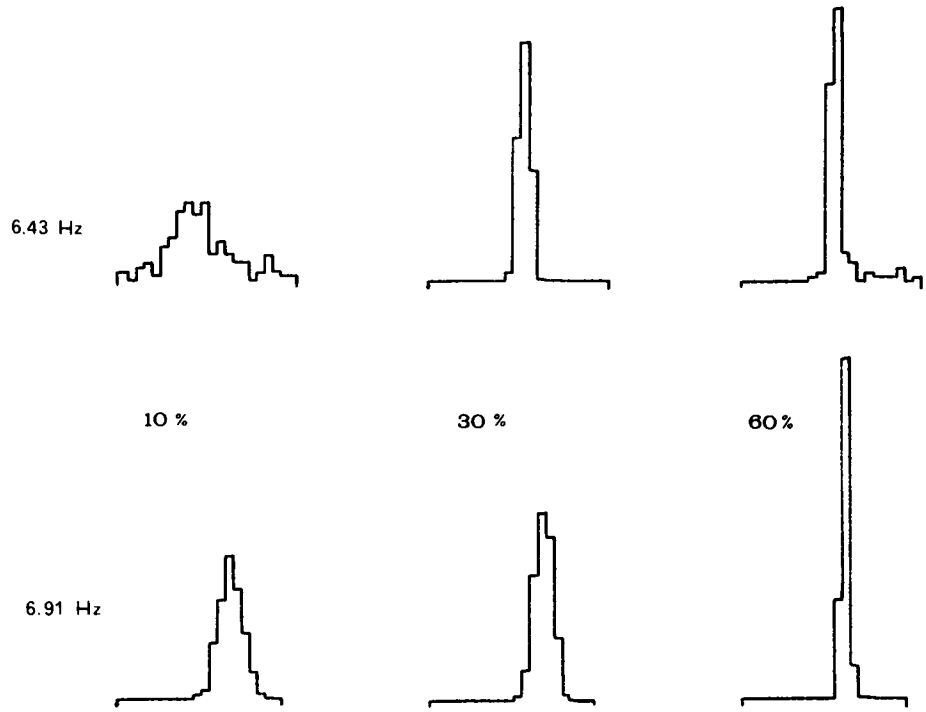

FIGURE 9 Cycle histograms of the responses of a retinular cell to light modulated at two different frequencies with the quoted modulation depths. Free-run rate f_0 = 6.7 spikes/s. Time bin: 3 ms.

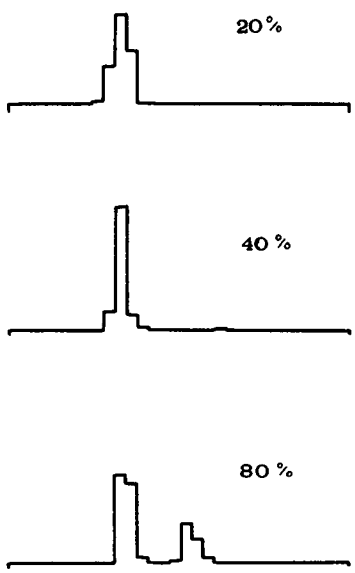

FIGURE 10 Cycle histograms of the responses of a retinular cell to light stimulation with three different modulation depths. f_0 = 3.2 spikes/s; ν = 3.4 Hz. Time bin: 10 ms.

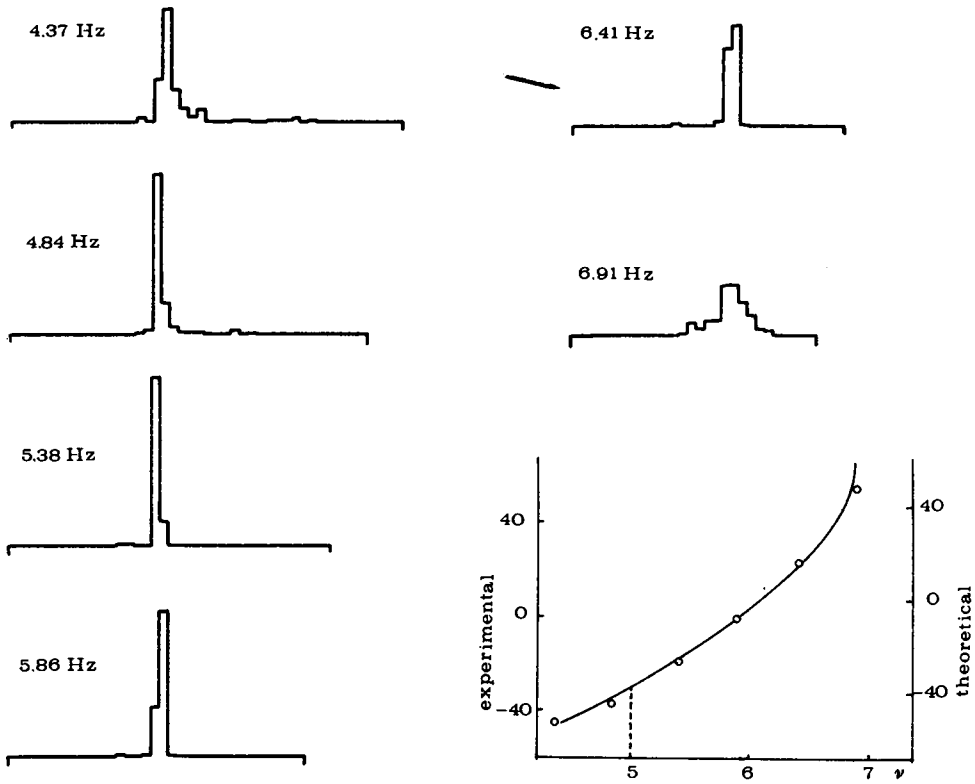

FIGURE 11 Cycle histograms of responses of an eccentric cell to 1.3 nA depolarizing current ($m = 0.2$). Insert: plot of measured φ vs. ν. The delay in detection of the spikes by the processor was taken into account. The fitting curve corresponds to $K = 1$, $\tau = 0.5$ s, $\gamma = 23\ s^{-1}$. Time bin: 5 ms.

predicted by the theory: the asymmetrical shape of the cycle histogram obtained at 6.43 Hz for the higher modulation depth clearly shows that the discharge is not really phase locked and measurement of the mean rate of discharge confirms that the firing rate entrainment is not complete in this case. Instead, for the higher stimulation frequency (6.91 Hz), an increase in the input modulation depth produces a narrowing of the peak in the cycle histogram. In general, the phase-locking condition is lost at suitable frequencies, as the stimulus modulation depth increases.

Fig. 10 refers to another cell where this effect appears very clearly. Other data show that the loss of phase locking also occurs in the case of current stimulation.

Fig. 11 shows the cycle histograms of the responses of an eccentric cell stimulated with 1.3 nA depolarizing current at several frequencies around the free-run rate f_0 of about 5 spikes/s, while the insert is a plot of the estimated φ values vs. ν (the continuous curve is a theoretical fit which is explained below). Note the regular increase of φ with increasing ν, a feature occurring in all the experiments performed, and the frequency range asymmetry with respect to f_0 in the direction of high frequencies. The total phase excursion is about 100°.

TABLE I

Cell	Cell type	g.p. amplitude	Current intensity	f_0	$\varphi(f_0)$	
					Light	Current
		mV	*nA*	*spikes/s*		
73/1	R	4	3	5.3	−50	+ 6
73/4	R		1.2	5.		− 3
74/19	R	7	h	7.	−75	0
75/2	R		1	7.		−15
75/2	R		0.5	4.		−20
75/3	R	5	h	5.9	−54	+ 5
75/5	R	5	h	7.	−65	0
75/6	R	4	—	2.3	−80	
74/16	E		1.3	5.		−32
74/18	E		1	8.8		−34
74/18	E		0.5	6.7		−34

R, retinular; E, eccentric; h, hybrid stimulation.

Tables I and II give some quantitative data for light and/or current stimulation in several cells. The phase of the locked spikes at the free-run frequency, $\varphi(f_0)$, which appears in the last column of Table I, was obtained by interpolation between the estimated phases at the nearest frequencies used.

One result is clear from Table I—there is a systematic discrepancy between the values of $\varphi(f_0)$ obtained with light or current stimulation in retinular cells. The

TABLE II

Cell and stimulation type		f_0	Variation coefficient	m	$\Delta\varphi$	$\varphi'(f_0)$	γ ($K = 1$)	γ ($K = 2$)
		spikes/s			°	°/*Hz*		
73/1	c		0.24	0.05	60	90		
		5.3					25	35
	l		0.12	0.06	90	65		
73/4	c	5	0.21	0.22	60	60	14	17
74/19	l		0.1	0.15	80	50		
		7					20	25
	h		0.1	0.15	70	45		
75/2	c	7	0.05	0.075	110	75	25	30
	c	4	0.05	0.15	120	65	15	18
75/3	l		0.23	0.15	45	45		
		5.9					21	26
	h		0.22	0.10	75	60		
75/6	l	2.3	0.35	0.2	40	25	25	30
74/16	c		0.035	0.22	90	30		
		5					23	30
	c		0.035	0.1	100	50		
74/18	c	8.8	0.055	0.2	90	50	20	23
	c	6.7	0.065	0.2	100	58	16	19

Abbreviations as in Table I.

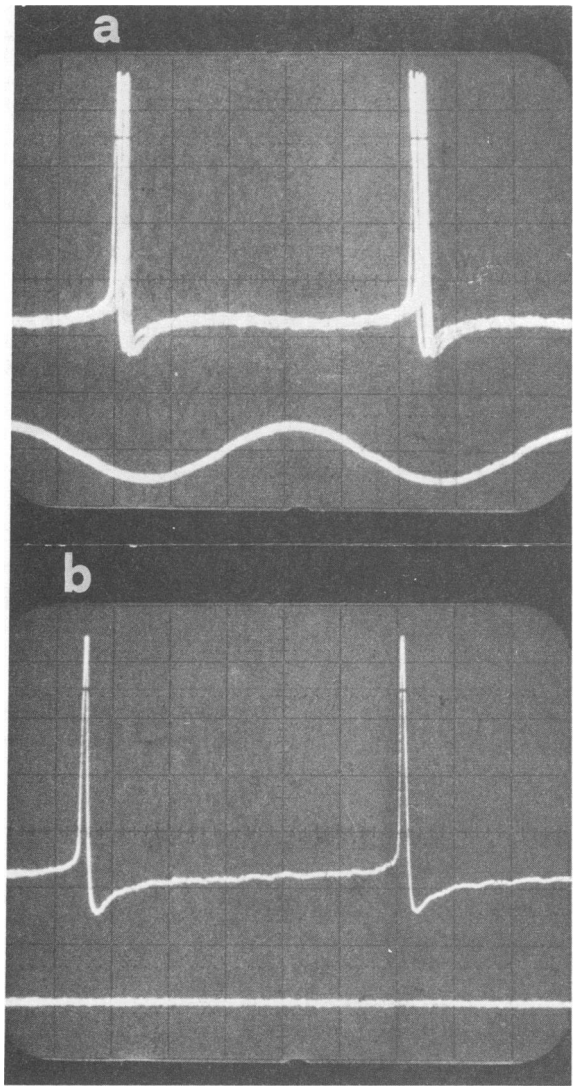

FIGURE 12 *a*. Phase-locked pattern recorded from an eccentric cell stimulated by light with 50% modulation depth; *b*. free discharge pattern at the same level of light.

first group have a large negative value, while the second are near zero. This finding will be discussed below.

In recordings from eccentric cells, the comparison between the two stimulation methods is not easy, the generator potential modulation being masked by the after-spike hyperpolarization (Fig. 12). By current stimulation in eccentric cells, we found values of $\varphi(f_0)$ intermediate between those obtained in retinular cells with light or current stimulation (see the last three rows of Table I).

In Table II we report other relevant parameters for the same cells reported in

Table I. The third column shows the variation coefficient, defined as the ratio between the standard deviation and the mean value of the interspike intervals, and giving a measure of the amount of noise in the discharge. This coefficient varies from one cell to another and is strongly influenced by the adaptation state of the cell. For instance, a dark-adapted cell normally has a variation coefficient much larger than the same cell in light-adapted conditions (see cell 73/1). The modulation depth m reported in the fourth column concerns the generator potential in the case of light stimulation; with current stimulation, it is simply the modulation depth of the current injected into the cell; in the case of hybrid stimulation, m is calculated as described in Methods.

The total phase excursion $\Delta\varphi = \varphi(\nu_{max}) - \varphi(\nu_{min})$ (using the same notations as under the Theory) is reported in the fifth column.

There are some difficulties in evaluating $\Delta\varphi$; the noise broadens the peaks in the cycle histograms at modulation frequencies near the limits of the locking range. The discharge is still considered phase locked if this broadening is not excessive and if the interval histograms are not bimodal. The $\Delta\varphi$ values so obtained vary from one cell to another and with the input modulation depth, but they appear to be independent of the type of stimulation and cell; their mean value is about 80°. Moreover $\Delta\varphi$ is lower for the cells with higher variation coefficient. This point will be discussed below.

In the sixth column of Table II we report the slope $\varphi'(f_0)$ of the curve $\varphi(\nu)$ for $\nu = f_0$, estimated as the ratio of the induced phase variation of the locked spikes to the difference in frequency between the two stimulation frequencies nearest f_0. The last two columns give the γ values by which the model reproduces the experimental slope at f_0. These values depend obviously on the values of the self-inhibition parameters K and τ; we have given them realistic values: 1 and 2 for K and 0.5 s for τ (Knight et al., 1970). The feasibility of fitting the model to these experimental data and the meaning of such a fit are discussed below.

THEORETICAL ANALYSIS AND DISCUSSION

Let us summarize here the main features of the experimental data reported above: (*a*) the phase at the free-run rate f_0 is, within the limits set by experimental error, independent of m; (*b*) the frequency range where the phase locking occurs is often not centered on f_0, but is displaced towards high frequencies, and the phase excursion is generally below 100°; (*c*) there are frequencies at which an increase in the input modulation depth destroys phase locking. All these features are present in the behavior of the self-inhibited leaky integrator model investigated under Theory. The next step would be to fit the estimated φ values for the various stimulation frequencies used in each experiment to the theoretical curve $\varphi(\nu)$. Now it is worth noting that, for the locking phase at the free-run frequency, Eq. 7 yields: $\varphi(f_0) = \tan(2\pi f_0/\gamma) - \pi/2$, independent of m and of the self-inhibition strength coefficient K. Thus the leakage constant γ should be immediately evaluated by measuring $\varphi(f_0)$. Unfortunately, the systematic discrepancy between the $\varphi(f_0)$ values obtained with different types of stimulation in retinular cells makes them unusable for this purpose. However, the

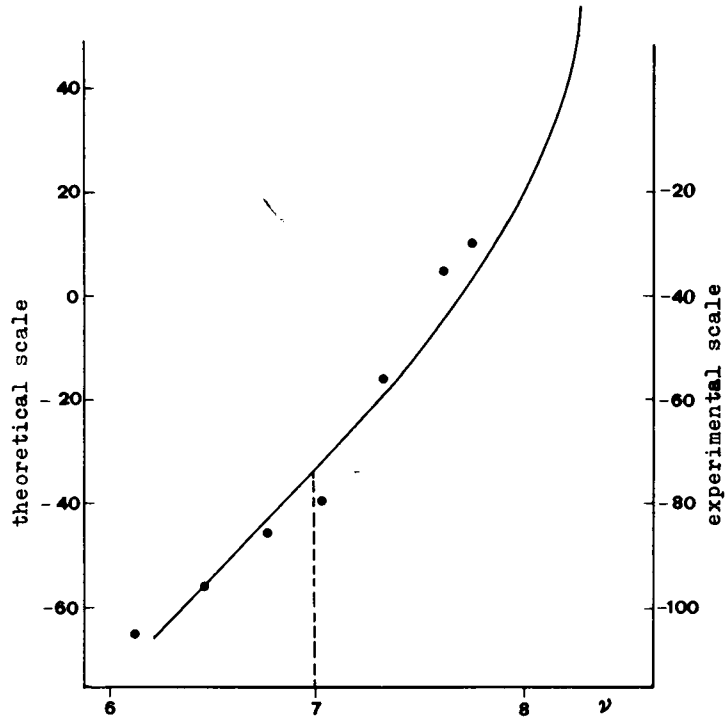

FIGURE 13 φ values measured in one retinular cell, 30% light-stimulated at several frequencies. The generator potential modulation depth was estimated 14% in all the range. $f_0 = 7$ spikes/s. The fitting curve corresponds to the model parameters: $K = 2$, $\tau = 0.5$ s, $\gamma = 30\ s^{-1}$.

model could still reproduce the *trend* of the experimental phases against the stimulation frequency, regardless of the numerical values of the phases. In Figs. 13 and 14 we report the experimental phases obtained from the retinular cell 74/19 and the fitting curves by the model. Note that the theoretical and experimental scales are shifted by a different amount for light or current stimulation. In this fit we have assumed the value 2 for the self-inhibition strength coefficient K and 0.5 s for the decay constant τ of self-inhibition. These are acceptable values of K and τ, as can be seen from the responses to steps of current (see for instance Fuortes and Mantegazzini, 1962) and from the transfer functions (Dodge, 1968; Knight et al., 1970). For the leakage constant we have used the value 30 s^{-1}. This value of γ, as shown by a previous paper (Barbi et al., 1975), is not too high to be compatible with the data reported for transfer functions and yields a good fit to our experimental data.

In Table II we have reported the γ values yielding the right slopes $\varphi'(f_0)$. Although these values are only indicative, because the best fit to the whole of the experimental data could occur for slightly different γ values, yet they give a useful indication of the possible values of γ. They range between 15 and 30 s^{-1} with the assumed values for the other parameters of the model (K and τ). It is worth noting that the values of γ

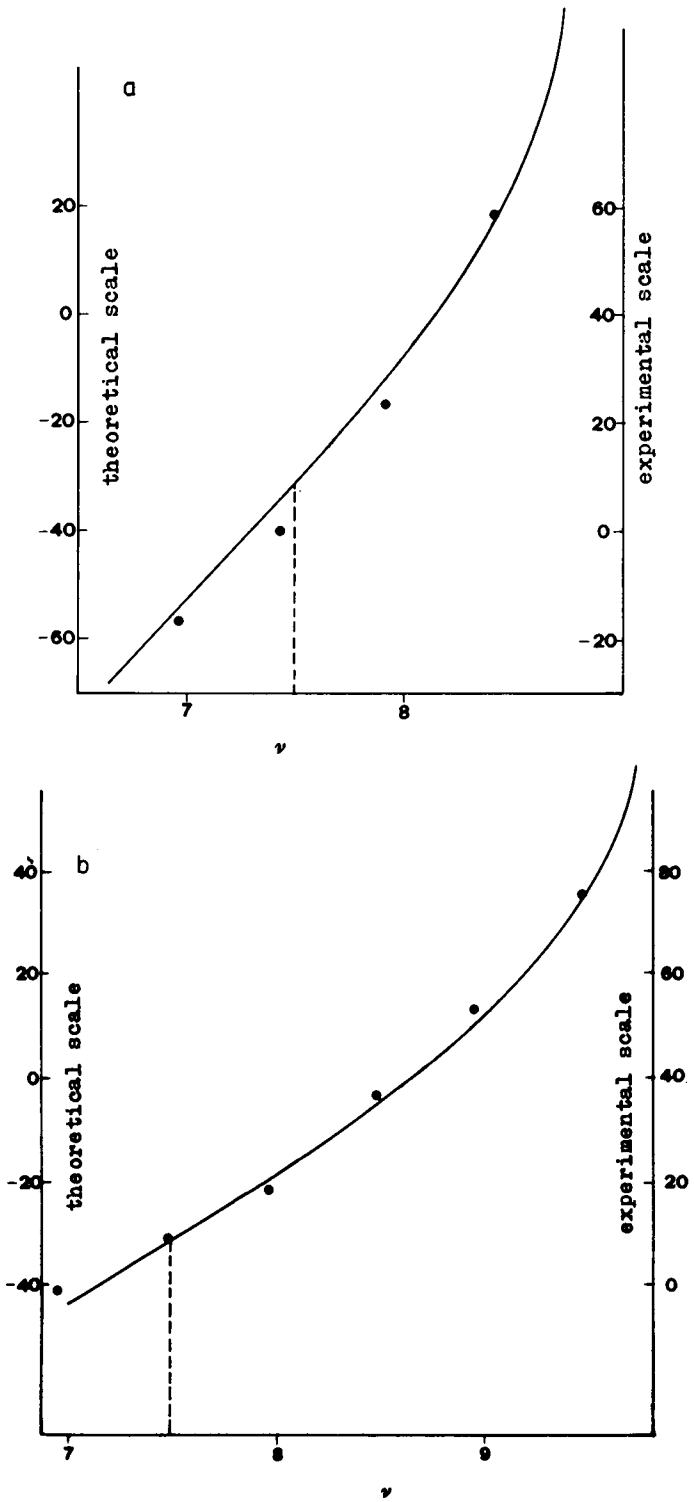

FIGURE 14 φ values measured in the same cell as in Fig. 13, but current stimulated. (I = 1 nA). The current modulation depth was 14% in *a*, 28% in *b*. f_0 = 7.5 spikes/s. Fitting curves correspond to the same model parameters as reported in Fig. 13.

obtained in this way coincide for light and current stimulation (see cell 73/1), and no systematic differences appear between the two types of stimulation. On the other hand, these γ values yield phase excursions $\Delta\varphi$ generally greater than the experimental ones. This can be accounted for by the noise affecting the discharge. In fact, by simulating a noisy discharge with an electronic analogue of the leaky integrator, we saw that the estimates of $\Delta\varphi$ obtained by the same criterion as in the experimental case are lower (by about 30° for a variation coefficient of 0.2) than the $\Delta\varphi$ obtained when there is no noise.

Coming back to the nonequivalence of light and current stimulation, we have found in retinular cells, it can be ascribed to the capacitive couplings of ommatidial cells. In fact, if capacitances play a role in the electrical connections between these cells, a difference must be expected between light stimulation (which affects all retinular cells in the ommatidium uniformly, thus annulling the effect of the capacitances between them) and current stimulation, which acts selectively on the impaled cell. In this context the comparison of generator potentials simultaneously recorded from retinular and eccentric cells in the same ommatidium would clarify a possible filtering action of the junction between these cells. A difference between light and current stimulation may be expected to appear also in recordings from eccentric cells, but this would be much lower than that occurring in retinular cells, due to the rectifying properties of the eccentric-retinular electrical junction (Smith and Baumann, 1969). The small shift between the theoretical and experimental scales we found by fitting the locking phases obtained from current-stimulated eccentric cells (see Fig. 11) confirms this inference. Moreover, experimental evidence of the equivalence of light and current stimulation in the eccentric cell has been obtained by measuring there the transfer functions of the encoding process by both methods of stimulation (Knight et al., 1970). Phase-locking analysis would probably yield a more precise test of that equivalence than that obtainable from transfer function measurements, but the phase measurements with light stimulation are difficult for the disclosed reasons.

As a final remark, the γ values reported in Table II do not show on the whole a clear correlation to the firing rate f_0, whereas this occurs in the crayfish stretch receptor neuron (Fohlmeister et al., 1974). Yet the cells where phase-locked responses have been recorded at two different levels of excitation show an increase of γ with increasing firing rate. However, our data do not give a conclusive answer to this problem.

APPENDIX

Let us call $Y(\nu)$ the right hand side of Eq. 5:

$$Y(\nu) = (\sqrt{\gamma^2 + \omega^2}/\gamma m)\left[\frac{(1 - e^{-\gamma/f_0})}{(1 - e^{-\gamma/\nu})} - 1\right],$$

whence: $Y(0) = -(1/m)\, e^{-\gamma/f_0}$.

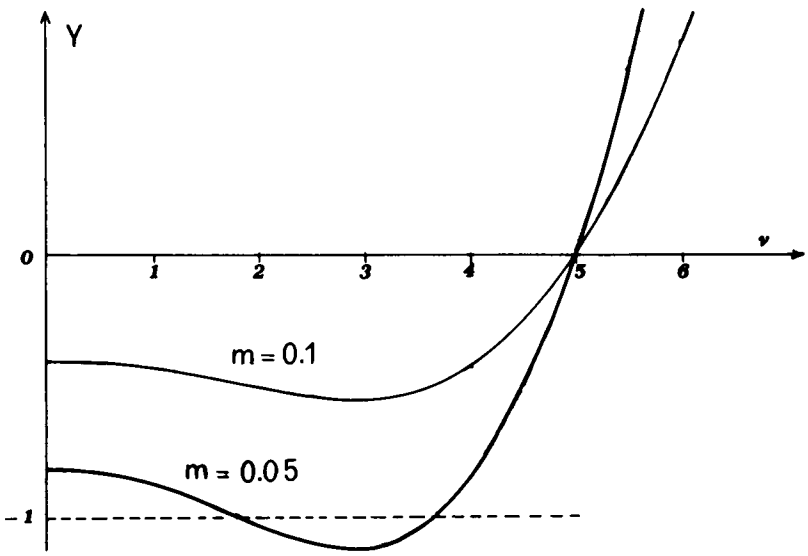

FIGURE 15 $Y(\nu)$ function. Parameter values: $f_0 = 5$ spikes/s, $\gamma = 16\ s^{-1}$.

The $Y(\nu)$ first derivative is given by:

$$Y'(\nu) = \frac{2\pi\omega}{\gamma^2 + \omega^2} Y(\nu) + \frac{\sqrt{\gamma^2 + \omega^2}}{m\nu^2} \frac{\frac{\gamma C}{s_0} e^{-\gamma/\nu}}{(1 - e^{-\gamma/\nu})^2},$$

yielding $Y'(0) = 0$; further computations show that $Y''(0) < 0$.

Thus $Y(\nu)$ starts at $\nu = 0$ with zero slope and then decreases.

Moreover, $Y(\nu)$ is the product of two monotonically rising functions of ν, the first positive and the second vanishing for $\nu = f_0$; that suggests that $Y(\nu)$ first decreases, reaching a negative minimum, and then always increases, vanishing for $\nu = f_0$. Fig. 15 plots the typical trend of the function $Y(\nu)$, numerically computed for the parameter values $\gamma = 16\ s^{-1}$, $f_0 = 5$ spikes/s, and two values of m (quoted). Now, if m is less than the value $m_{crit} = 1 - \gamma C/s_0$, it is $Y(0) < -1$, and the ν_{min} frequency is defined; $m < m_{crit}$ is also the sufficient condition for the $u(t)$ monotonicity (see text). Moreover, let us call m^* the m value ($>m_{crit}$) at which the $Y(\nu)$ minimum equals -1. Since the phase-locking condition cannot hold at zero frequency, for $m > m^*$ the relative maximum of $u(t)$ within the time interval $(0, \nu^{-1})$ will reach the firing threshold for a modulation frequency that is actually the lower end of the phase-locking range. In fact, as we checked by numerical computations, this effect begins for an m value intermediate between m_{crit} and m^*.

Received for publication 28 July 1976 and in revised form 25 April 1977.

REFERENCES

ASCOLI, C., M. BARBI, C. FREDIANI, G. GHELARDINI, and D. PETRACCHI. 1974. Rectification and spike synchronization in the *Limulus* lateral eye. *Kybernetik.* **14**:155.

ASCOLI, C., M. BARBI, S. CHILLEMI, and D. PETRACCHI. 1976. Phase locking of neural discharge to peri-

odic stimuli. Proceedings of the Third European Meeting on Cybernetics and Systems Research. R. Trapple, editor. Hemisphere Publishing Corporation, Washington, D.C.

BARBI, M., V. CARELLI, C. FREDIANI, and D. PETRACCHI. 1975. The self-inhibited leaky integrator: transfer functions and steady-state relations. *Biol. Cybern.* **20**:51.

BAYLY, E. J. 1968. Spectral analysis of pulse frequency modulation in the nervous systems. *IEEE (Inst. Electr. Electron. Eng.) Trans. Biomed. Eng.* **15**:257.

DODGE, F. A. 1968. Excitation and inhibition in the eye of *Limulus*. In Optical Data Processing by Organisms and Machines. W. Reichardt, editor. Academic Press, Inc. New York. 341.

FOHLMEISTER, J. F., R. E. POPPELE, and R. L. PURPLE. 1974. Repetitive firing: dynamic behavior of sensory neurons reconciled with a quantitative model. *J. Neurophysiol.* **37**:1213.

FRENCH, A. S., A. V. HOLDEN, and R. B. STEIN. 1972. The estimation of the frequency response function of a mechanoreceptor. *Kybernetik.* **11**:15.

FUORTES, M. G. F., and F. MANTEGAZZINI. 1962. Interpretation of the repetitive firing of nerve cells. *J. Gen. Physiol.* **45**:1163.

KNIGHT, B. W. 1969. Frequency response for sampling integrator and for voltage to frequency converter. *In* Systems Analysis in Neurophysiology. C. A. Terzuolo, editor. Brainerd. Minn.

KNIGHT, B. W. 1972*a*. Dynamics of encoding in a population of neurons. *J. Gen. Physiol.* **59**:734.

KNIGHT, B. W. 1972*b*. The relationship between the firing rate of a single neuron and the level of activity in a population of neurons. *J. Gen. Physiol.* **59**:767.

KNIGHT, B. W., J. TOYODA, and F. A. DODGE. 1970. A quantitative description of the dynamics of excitation and inhibition in the eye of *Limulus*. *J. Gen. Physiol.* **56**:421.

POPPELE, R. E., and R. J. BOWMAN. 1970. Quantitative description of linear behavior of mammalian muscle spindles. *J. Neurophysiol.* **33**:59.

POPPELE, R. E., and W. J. CHEN. 1972. Repetitive firing behavior of mammalian muscle spindles. *J. Neurophysiol.* **35**:357.

PURPLE, R. L., and F. A. DODGE. 1965. Interaction of excitation and inhibition in the eccentric cell in the eye of *Limulus*. *Cold Spring Harbor. Symp. Quant. Biol.* **30**:529.

RESCIGNO, A., R. B. STEIN, R. L. PURPLE, and R. E. POPPELE. 1970. A neural model for the discharge patterns produced by cyclic inputs. *Bull. Math. Biophys.* **32**:337.

SMITH, T. G., and F. BAUMANN. 1969. The functional organisation within the ommatidium of the lateral eye of *Limulus*. *Prog. Brain Res.* **31**:313.

STEIN, R. B., A. S. FRENCH, and A. V. HOLDEN. 1972. The frequency response, coherence, and information capacity of two neuronal models. *Biophys. J.* **12**:295.

STEVENS, C. F. 1964. A quantitative theory of neural interactions: theoretical and experimental investigations. Thesis. The Rockefeller University.

TOMITA, T. 1957. Peripheral mechanism of nervous activity in lateral eye of horseshoe crab. *J. Neurophysiol.* **20**:245.